

# Fractional Derivatives Applied to Phase Space Reconstructions<sup>1</sup>

B. F. Feeny

*Michigan State University  
Department of Mechanical Engineering  
East Lansing, MI 48824 USA, feeny@egr.msu.edu*

G. Lin

*Department of Electrical Engineering  
University of Maryland  
University Park, MD, linguoji@umd.edu*

## Abstract

The concept and application of phase-space reconstructions are reviewed. Fractional derivatives are then proposed for the purpose of reconstructing dynamics from a single observed time history. A procedure is presented in which the fractional derivatives of time series data are obtained in the frequency domain. The method is applied to the Lorenz system. The ability of the method to unfold the data is assessed by the method of global false nearest neighbors. The reconstructed data is used to compute recurrences and correlation dimensions. The reconstruction is compared to the commonly used method of delays in order to assess the choice of reconstruction parameters, and also the quality of results.

## 1 Introduction

When doing experiments with dynamical phenomena, it is not always possible to sense all of the active states in the system. A *phase space reconstruction* can often be used to rescue the experimenter in this situation.

A phase-space reconstruction is the extraction of the full dynamics of a system from a small number of observables. The goal of a phase-space reconstruction is to take, typically, a single sampled measurement history and view it in a higher-dimensional space, which can somehow accommodate the dynamics that generated the signal. If successful, there is a one-to-one relationship between data in the reconstructed phase space, and associated data in the true state space. Loosely speaking, in this case the reconstruction is called an *embedding*. The fully reconstructed state space (or the embedding) is useful in system characterization, nonlinear prediction, and in estimating bounds on the size of the system [1, 2].

One reconstruction idea has been to use derivatives of the sampled quantity [3, 4]. This idea might be motivated by the usage of displacement and velocity as states in oscillators. Takens has proven that this method will produce embeddings, provided that the system

---

<sup>1</sup>*Nonlinear Dynamics* **38** (1-4) 85-99 (2004), Special Issue on Fractional Calculus

is sufficiently smooth and noise free (see also Noakes [5]). However, real systems are not noise-free. The successive derivatives of the observed state are prone to increasing noise amplification as the order of the derivative increases.

By far the most common method of phase-space reconstruction is the method of delays [3, 4]. Details about the method of delays are presented shortly.

In this paper, we propose the usage of fractional derivatives for the purpose of phase-space reconstructions of data from nonlinear dynamical systems.

In what follows, we briefly provide background on phase-space reconstructions. We summarize the fractional derivative, and its application by using the fast Fourier transform (FFT). We then outline the application of fractional derivatives to time-series data. The fractional derivatives are applied to reconstruct the phase space in an example, and then compared to the reconstruction obtained by the more common method of delays. The correlation dimension and recurrence behavior are examined in the reconstruction data. Conclusions are then drawn.

## 2 Background on Phase-Space Reconstructions

In this section, we review the methods for reconstructing the phase space from a single observable, and also other computations done for proper reconstructions of the phase space, and characterizing the dynamics. First we look at details of the method of delays. Understanding the method of delays provides some insight to what might be needed in a fractional-derivative phase-space reconstruction.

### 2.1 The Method of Delays

The method of delays, introduced independently in references [3, 4], is the most common method for reconstructing the phase space. Suppose we have a measurement  $y$  which is essentially a smooth function of the states  $\mathbf{x}$ , i.e.  $y = f(\mathbf{x})$ . Suppose further that the states evolve in time  $t$ , and the measurement is sampled at a sampling interval  $\Delta t$ , generating a series of quantities  $y_n$ , with  $n = 1, \dots, M$ . According to the method of delays, we build vectors  $\mathbf{y}_n = (y_n, y_{n+h}, \dots, y_{n+(d_E-1)h})$ , where  $h$  is a delay index, and  $d_E$  is the dimension of  $\mathbf{y}_n$ . The delay time is  $\tau = h\Delta t$ . The *pseudo vectors*  $\mathbf{y}_n$  can then be plotted in a  $d_E$ -dimensional space. The sequence of points  $\mathbf{y}_n$  traces out a sampled curve in this *pseudo phase space*. This forms the reconstructed phase space, in which the next stage of data analysis and modeling can be pursued.

The method of delays can be intuitively justified by considering that the delay coordinates represent a linear transformation from coordinates that represent finite differences in time. Since mechanical systems have states which can be represented by displacements and velocities, the choice of discretized derivatives as pseudo states seems like a natural one. Incidentally, derivatives of the observable have also been considered for performing reconstructions [3, 4], and while this idea does produce a pseudo phase space in theory, it has the problem of noise amplification, and is not considered practical.

The method of delays has been justified for smooth systems by 'Takens' embedding

theorem [3], which states that, if basic hypotheses are satisfied, applying the method of delays to an observable produces a trajectory in the reconstructed or pseudo phase space which is a *topological embedding* of the trajectory in the real phase space. The important meaning of this is that the limit set in the real space is mapped injectively to the reconstructed phase space.

Among the basic hypotheses is that the embedding dimension must be known. That is, when the method of delays is performed, the choice of  $d_E$  must be large enough to accommodate the dynamics. Furthermore, as it turns out, because of the presence of uncertainty and noise in the system, the choice of the delay index or delay time  $\tau$  must be carefully made. We briefly discuss these issues next.

## 2.2 Choosing the Delay Time

In an ideal, noise-free setting, almost any time delay can be used in the phase-space reconstruction. However, the presence of noise makes the choice of the delay time an important one. If the delay is too small, then the elements of the pseudo vectors become too similar, such that the pseudo vectors tend to lie on a diagonal in the space, and the reconstruction does not produce much information. On the other hand, since the reconstruction is often performed on a system with complicated dynamics, which often involve sensitive dependence on initial conditions, the usage of an excessively large time delay leads to pseudo vectors whose elements are largely uncorrelated, yielding a random-looking pseudo phase space. In this case, much information is lost, and the structure of the dynamics is difficult to ascertain.

Various methods have been proposed to choose an appropriate delay time [2]. One school of thought is to choose  $\tau$  based on the autocorrelation of the sampled observable. Intuitively, when the autocorrelation is minimal, the correlation between the observable and its delay is minimal, indicating that this delay, used to define coordinate axes, will lead to optimally independent axes. The problem is that autocorrelation is a linear operation, and we are generally dealing with nonlinear data. And while this method is often successful, there are some examples in which it generates unsatisfactory results [6, 7].

The preferred alternative is the average mutual information [8]. This is computed by plotting  $y_{n+h}$  against  $y_n$ , and dividing this two-dimensional delay space into square bins. Denoting  $A$  as the set corresponding to one axis, and  $B$  as the set corresponding to the other, we can then set event  $a$  to represent a bin in  $A$ , and event  $b$  to represent a bin in  $B$ . Then  $P_A(a)$  is the probability of  $a$  in  $A$ , which is the number of data in bin  $a$  divided by the total number of data, and  $P_B(b)$  is defined likewise.  $P_{AB}(a, b)$  is the joint probability, which equals the number of data that are in  $a$  and also in  $b$ , divided by the total number of data. In other words, the bins form a grid on the two-dimensional plot. Bin  $a$  is a vertical strip, and bin  $b$  is a horizontal strip.  $P_A(a)$  is obtained by counting data in the vertical and horizontal strips, and  $P_{AB}(a, b)$  is obtained by counting data in the intersection of the strips. Given these probabilities, then

$$I_{AB}(a, b) = \log_2 \frac{P_{AB}(a, b)}{P_A(a)P_B(b)}.$$

The average mutual information is then obtained by averaging this quantity over all the bins.

To find the best choice for a value of the delay index  $h$ , one computes the average mutual information for a range of delay indices, and chooses the first minimum. This provides coordinate axes that have minimal mutual information, and hence optimal independence, without excessively large delays. Indeed, it is possible for the average mutual information plot to show no local minimum, in which case the calculation can still provide a guide for the choice. Furthermore, this approach is used to seek independence between two adjacent reconstruction coordinates,  $y_n$  and  $y_{n+h}$ , while disregarding the independence between other coordinates,  $y_n$  and  $y_{jh}$ ,  $j = 2, \dots, d_E - 1$ .

## 2.3 Determining the Embedding Dimension

The embedding dimension is the dimension of the reconstruction if it is an embedding. A key property of the embedding is that the mapping from the real space to the pseudo space is one-to-one. If trajectories cross each other in the pseudo space, it is not an embedding.

The method of false nearest neighbors (FNN) has been developed to search through the data and identify the presense of trajectory crossings [1]. The idea is that if the embedding dimension is too small, portions of the strange limit set will cross over itself. As an example, suppose a warped closed curve in three dimensions is projected into two dimensions such that it forms a figure-eight. The figure-eight has a crossing point. But when expanded back into three dimensions, the curve can “unfold” and bypass this crossing point.

Thus, as the dimension of the reconstruction is increased, these false crossings unfold. So if the nearest neighbor of a pseudo phase point reconstructed in dimension  $d$  suddenly becomes far away when the reconstruction dimension is increased, then it will have been considered a false nearest neighbor. In this work, a nearest neighbor is labeled “false” if  $R_{d+1}/R_d > 15$ , where  $R_d$  is the distance between the points in the  $d$ -dimensional reconstruction space. (There is a second FNN criterion for noisy data [1], which we need not apply in this work.) When a dimension is reached in which there are essentially no false nearest neighbors, then the appropriate embedding dimension is found.

This test can be applied after the appropriate choice of  $\tau$  has been made. Alternatively, one can plot the number of false nearest neighbors versus  $\tau$  and look for a robust choice of the embedding dimension  $d_E$ . A healthy reconstruction usually has some robustness in the determination of the embedding dimension  $d_E$  under variations in other parameters, such as the delay time.

## 2.4 Other Phase-Space Reconstructions

Distortions of the method of delays have been documented, for example by Potopov [10] and Mindlin [11]. An inherent issue is that any point in the reconstructed phase space is represented by a finite time interval,  $[t, t + (d_E - 1)\tau]$ , as opposed to an instant of time in the true phase space. In contrast, the derivatives method of reconstructions establishes reconstruction vectors that truly correspond to instants in time, but has noise amplification problems. Stick-slip systems also cause problems in the method of delays [12] and the method of derivatives. Although these methods were not proven for nonsmooth systems [3], needed for a stick-slip process, it is possible for the methods to be unknowingly applied.

As an alternative to delay and derivative phase-space reconstructions, a mix of integrals and derivatives has been suggested [13, 14]. The presence of an integral can introduce a drift in the reconstruction. For example, a periodic orbit with a constant component in the original space will not be periodic in the reconstructed space due to the integration of a constant component in the periodic orbit. Hence the reconstructed phase space with a purely integrated component is qualitatively different than the true phase space; it is generally not one-to-one, and hence cannot be an embedding. Gilmore and Lefranc [14] suggest removing the mean of the signal to avoid such secular behavior. High-pass filtering might also be an option [15].

In this work, we propose the reconstruction the phase space by using *fractional derivatives*. We will show evidence, in an example, that fractional derivatives produce independent coordinates in the reconstructed phase space. Also, a fractional derivative can be incremented several times before accumulating a large order to the total derivative. Thus, it is possible to obtain a moderate number of dimensions in the reconstructed phase spaces of low-noise systems without excessive amplification of the noise. The fractional derivative is easy to apply to time series. Points in the resulting reconstruction space are seemingly represented by time instants as opposed to time intervals. However, those who have performed numerical integrations of fractional-order differential equations know that the dynamical history is involved (more on this later).

## 2.5 Characterizing the Data in the Reconstructed Phase Space

Since a properly reconstructed phase space *qualitatively* represents the dynamics of the true phase space, the data analyst can perform all sorts of computations on the reconstructed data to characterize the system in some meaningful way. For example, Lyapunov exponents and fractal dimensions can be calculated or the recurrence behavior can be examined. Nonlinear prediction methods or system identification can be applied. In low-dimensional cases, the dynamic attracting set can be visualized by looking at the Poincaré section.

In this paper, we will look at recurrence behavior and correlation dimensions.

Recurrences are often used for extracting the unstable periodic orbits from a chaotic attractor. The idea is, given a reconstruction, we look for near periodicities by examining the distance between a point  $\mathbf{y}_n$  and its iterates  $\mathbf{y}_{n+k}$ . If  $\|\mathbf{y}_n - \mathbf{y}_{n+k}\| < \epsilon$ , where  $\epsilon$  is some prescribed small value, then the points are considered to be part of a nearly periodic trajectory of period  $kh$ . For example,  $\epsilon$  might be taken as 0.005 times the span of the attractor [16–18]. We can plot the number of recurrences versus  $k$ . In a smooth system, the recurrence plot shows spikes at values of  $k$  corresponding to the periods of the unstable periodic orbits that are visited. We can also look at the data for the span of indices for which a recurrence takes place, i.e. on the interval of data that is considered to be approximately periodic. The collection of unstable periodic orbits might be used for determining determinism, estimating the fractal dimension [19] or Lyapunov exponents [16], or identifying system parameters [20–23].

Fractal dimensions are sometimes used to estimate the dimension of the attracting set. Common measures of dimensions are the limit capacity, information dimension, and correlation dimension [24]. It is also possible for an entire spectrum of dimensions, or the

multifractal spectrum [25], to be calculated [26]. We will apply correlation dimension calculations [27] in our example.

To compute the correlation dimension, we first calculate the correlation integral,

$$C(r) = \frac{1}{N^2} \sum_{i \neq j}^N \sum_{j=1}^N u(r - |\mathbf{x}_i - \mathbf{x}_j|), \quad (1)$$

where  $u$  is the heaviside (step) function ( $u(z) = 0, z < 0, u(z) = 1, z \geq 0$ ) and  $r$  is a specified “ball” size. In other words,  $C(r)$  is the number of pairs of data  $\mathbf{x}_i$  and  $\mathbf{x}_j$  with  $|\mathbf{x}_i - \mathbf{x}_j| \leq r$ , divided by  $N^2$ . Locally,

$$C_i(r) = \frac{1}{N} \sum_{j=1}^N u(r - |\mathbf{x}_i - \mathbf{x}_j|),$$

is the normalized ( $1/N$ ) number of points  $\mathbf{x}_j$  that are  $r$ -close to the reference data  $\mathbf{x}_i$ . Then  $C(r)$  is the mean of the  $C_i(r)$ . To ease the computational effort, it might be reasonable to estimate the mean of the  $C_i(r)$  by randomly selecting a subset of  $M$  (where  $M \ll N$ , but is still a large number) reference points  $\mathbf{x}_i$  [28, 29], which is how we do the computation in this work.

Given  $C(r)$ , the correlation dimension  $d_c$  is obtained by presuming  $C(r) \sim r^{d_c}$  as  $r \rightarrow 0$ . Thus,  $\log C(r) \sim d_c \log r$ . Since it is not feasible to take  $r \rightarrow 0$  for finite data sets, the idea is to seek a linear scaling region for small  $\log r$  in the  $\log C(r)$  versus  $\log r$  plot, and take the slope as the correlation dimension  $d_c$ .

Poincaré sections are basically cross-sections of the phase space. As continuous-time trajectories pierce the Poincaré section, they define points on the Poincaré section. The sequence of points are mapped on the Poincaré section according to the flow of the trajectories in the full phase space. the dimension of the attractor in the full phase space is  $d_c = 1 + d_c^P$ , where  $d_c^P$  is the dimension in the Poincaré section.

In this paper, we will reconstruct a chaotic data set using the method of fractional derivatives, and also using the method of delays and the true phase space for reference. We will characterize the dynamics using the above measures, and compare the results for the different phase spaces.

## 3 Fractional Derivatives

### 3.1 Background

Example applications of fractional derivatives include visco-elasticity models in oscillators [30–32], flows through porous media [33], and the characterization of fractal functions [34]. In the modeling examples, fractional derivatives appear as terms in the differential equations of motion, or equivalently as fractional power terms in the denominator of a transfer function.

The Liouville-Riemann fractional derivative can be expressed for non-integer order  $a < 0$  as

$$\frac{d^a x(t)}{d(t - t_0)^a} = \frac{1}{\Gamma(-a)} \int_{t_0}^t \frac{x(\tau)}{(t - \tau)^{a+1}} d\tau, \quad (2)$$

where  $t_0$  suggests an initial condition, and plays a significant role in the integration process. For  $a > 0$ , one can apply

$$\frac{d^a x(t)}{d(t-t_0)^a} = \frac{d^n}{dt^n} \frac{1}{\Gamma(n-a)} \int_{t_0}^t \frac{x(\tau)}{(t-\tau)^{a-n+1}} d\tau, \quad (3)$$

for  $n > a$  [35]. Quite often,  $t_0$  is taken to be zero.

Our interest is in applying the fractional derivative to time-series data. This will not have been the first time for fractional differintegration of time series. The fractionally integrated autoregressive moving average (ARFIMA) has been applied as a time-series modeling and forecasting tool for long-memory processes, for example econometrics and hydrology [36, 37]. In our work, we perform fractional differentiation of the time series by first applying the Fourier transform, and then computing the fractal derivative in the frequency domain [38].

The fractional derivative is difficult to interpret in a spatial domain (in comparison to the familiar slope and curvature) and in the time domain (in comparison to velocity, acceleration, and jerk). However, in the frequency domain, we interpret derivatives of dynamic signals based on a scaling of the amplitudes and phase shifts of the signal's sinusoidal elements. The  $n^{\text{th}}$  derivative of a complex exponential of frequency  $\omega$  is represented by a multiplication by  $(i\omega)^n$ . That is, the amplitude is scaled by  $\omega^n$ , and the phase is shifted by  $n\pi/2$ . Accordingly, the fractional derivative of a sinusoid or complex exponential is easily interpreted as a scaling of the amplitude by a fractional power of the frequency, and a shifting of the phase by a fraction of  $\pi/2$ .

As such, in contrast to application of the fractional derivative according to the definition in equation (2), in the domain of the independent variable, the fractional derivative  $d^a x(t)/dt^a$  of fractional order  $a$  of a signal  $x(t)$  is easily computed in the frequency domain by taking the Fourier transform of the signal, multiplying by  $(i\omega)^a$ , and finally transforming back to the time domain [38]. It turns out that this representation is consistent with the fractional derivative of an exponential function [35],  $d^a x(t)/d(t-t_0)^a$ , as  $t_0 \rightarrow -\infty$ , meaning at steady state. Since our reconstructions are to be performed on chaotic data which are taken to be at steady state, this process is reasonable.

The “generalized derivative” is similar to the fractional derivative applied in the frequency domain. In the case of the generalized derivative, the signal is multiplied by  $i|\omega|^a$  in the frequency domain [14]. For the case of  $a = 0$ , the generalized derivative corresponds to the Hilbert transform. Gilmore and Lefranc [14] applied the generalized derivative to data from a dynamical system and used it to make plots resembling a two-dimensional phase portrait.

We apply the fractional derivative in the frequency domain for the purpose of phase-space reconstruction, using the fast Fourier transform (FFT) for computational feasibility. Since the FFT has some approximation built in, we will refer to the computed fractional derivative of a signal  $x(t)$  as  $D^a x(t)$ , in lieu of the true fractional derivative  $d^a x(t)/dt^a$ .

## 3.2 Leakage

When using the FFT, its problems are inherited. A problem that takes our attention is leakage. Leakage results because the FFT algorithm looks at an infinitely long time series

built by repeating the finite time series data ad infinitum. Splicing the finite time record to itself produces discontinuities at the splices, which distort the frequency domain information through Gibbs phenomenon.

In the time domain, leakage is apparent as transient Nyquist-frequency oscillations near the endpoints of the signal after applying the FFT to the time record, manipulating in the frequency domain, and then inverting the FFT. Examples of this effect can be seen in references [14, 15].

A common way to deal with leakage in linear signal analysis is to multiply the time record by a windowing function, which typically smoothly changes from zero to one, and back to zero by the end of the time record [39]. In this paper we use the terminology “windowing” to describe the use of a windowing function. Windowing is an excellent treatment in linear signal analysis, when the interest is in frequency content. However, in nonlinear signal analyses, such as the phase space reconstruction, the aim is to preserve the geometry of the dynamics. Windowing distorts the geometry. For example, chaotic data continually visits unstable periodic orbits (UPOs). If we choose to extract the UPOs, a windowed time record will yield distorted UPOs. For instance, how two different UPOs are linked may not be preserved if the time record is windowed.

Therefore, we do not use windowing to treat leakage here. Instead, since the distortion due to leakage is at the endpoints of the time series, affecting a small percentage of the data, we will *truncate* the time record to remove the effect of leakage. To determine where to truncate the data, we obtain  $\dot{x}(t)$  from finite differences, perhaps with low-pass filtering if necessary, and  $Dx(t)$  by using the frequency domain. For each time sample, we examine  $\delta(t_n) = |Dx(t_n) - \dot{x}(t_n)|$ . We retain  $Dx(t_m)$  for the interior range of samples where  $\delta(t_n) < \epsilon$ , for some acceptable tolerance  $\epsilon$ . An example of this truncation error will be shown later. We assume that the leakage error is of similar magnitude for other fractional derivatives.

Another possible approach is to select a subset of the time series data for which the beginning and end points are nearly the same [14]. Perhaps a combined approach would be most robust.

The use of fractional derivatives for reconstructing the phase space is discussed next.

### 3.3 Phase-Space Reconstruction

The proposed protocol for using fractional derivatives to obtain pseudo phase coordinates for phase space reconstructions is as follows.

First, we have some computations that need be performed once:

1. Generate sampled time series data  $x(t_n)$  with a constant sampling rate.
2. Use the FFT of  $x(t_n)$  to obtain the data  $X(\omega_n)$  in the frequency domain.
3. Evaluate the post FFT leakage error by computing  $\delta(t_n) = |Dx(t_n) - \dot{x}(t_n)|$ , where  $Dx(t_n)$  is obtained from the inverse FFT of  $i\omega_n X(\omega_n)$  and  $\dot{x}(t_n)$  is obtained by finite differences.
4. Find the interior range of samples for which  $\delta(t_n) < \epsilon$  to guide the truncation of the fractal derivative signals.



We then perform the following computations for each pseudo coordinate  $D^{ma}x(t)$ ,  $m = 1, 2, \dots, d-1$ , of the reconstructed phase space:

1. In the frequency domain, compute  $D^{ma}X_n = (i\omega_n)^{ma}X_n$
2. Invert the FFT to obtain  $\hat{y}_{ma}(t_n) = D^{ma}x(t_n)$
3. Retain the  $\hat{y}_{ma}(t_n)$  for the interior range of samples for which  $\delta(t_n) < \epsilon$  (based on step 4 above).
4. We then normalize each axis of the data, such that  $y_{ma}(t_n) = \hat{y}_{ma}(t_n)/R_m$ , where  $R_m = \max_m(\hat{y}_{ma}(t_n)) - \min_m(\hat{y}_{ma}(t_n))$  is the span of the unnormalized coordinate  $\hat{y}_{ma}(t_n)$ . This normalization is for the benefit of the time series analysis metric characterization methods that involve finding data with small “balls.”

Then the  $d$ -dimensional reconstructed phase space vectors have the form

$$\begin{aligned}\mathbf{y}_n &= [y_0(t_n), y_1(t_n), y_2(t_n), \dots, y_{d-1}(t_n)] \\ &= \left[ \frac{x(t_n)}{R_0}, \frac{D^a x(t_n)}{R_1}, \frac{D^{2a} x(t_n)}{R_2}, \dots, \frac{D^{(d-1)a} x(t_n)}{R_{d-1}} \right].\end{aligned}$$

The value of  $a$  is a reconstruction parameter analogous to the delay index in the method of delays. Parameter  $a$  can be chosen with the help of an average-mutual-information computation between  $x(t_n)$  and  $D^a x(t_n)$ . In this work we do not seek a minimum average mutual information, but a balance between a low average mutual information, and a large derivative order  $a(d-1)$ . The value of  $d = d_E$  can then be determined [1, 9].

In this paper, we do not prove that  $\mathbf{y}_n$  is an embedding. However, in the next section, we perform phase space reconstructions on an example. We compare fractional-derivative reconstructions with delay reconstructions for reference. We will compute the embedding dimension  $d_E$ , the correlation dimension, and the recurrence behavior, and compare the results between the fractional derivative and delay reconstructions. It may be that these quantities have not yet been computed in an embedding not created by the method of delays [14]. Our example involves low-noise numerical data. The method has also been applied to “clean” experimental data [40]. Dealing with higher levels of noise will be a topic of future study.

## 4 Example: The Lorenz System

The equations of motion of the Lorenz system [41] are

$$\begin{aligned}\dot{x} &= \sigma(y - x), \\ \dot{y} &= rx - y - xz, \\ \dot{z} &= xy - bz,\end{aligned}\tag{4}$$

where  $\sigma = 10$ ,  $r = 28$ , and  $b = 8/3$ . The sampling time interval was  $\Delta t = 0.01$  for the numerical solution. We obtained 57344 samples in the observable  $x$ .

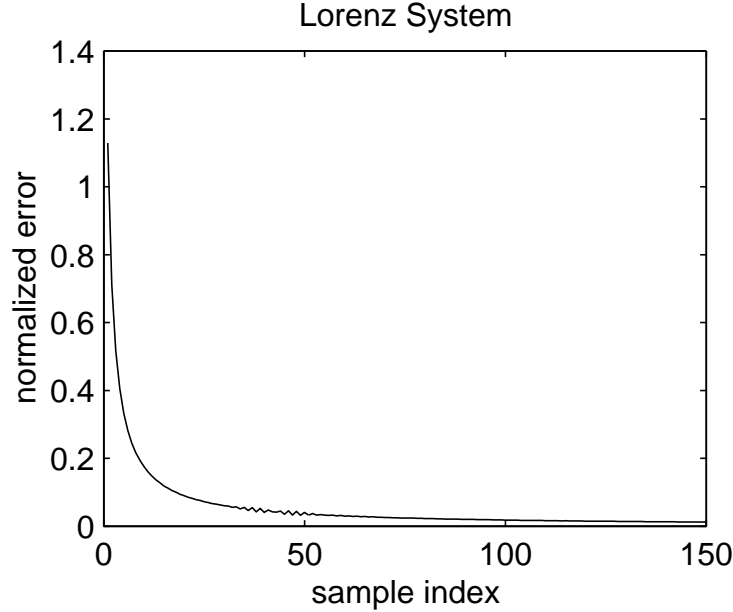


Figure 1: The normalized error between the velocities calculated in the frequency domain and by finite differences,  $|Dx - \dot{x}|/(\max \dot{x})$ , for the first 150 points of the numerical solution.

The phase space is to be reconstructed by means of fractional derivatives, and, for assessment of the reconstruction parameters, by means of the delay method for comparison.

In performing the fractional derivative reconstruction, we computed the fractional derivatives, and then removed the leakage effects by truncating 150 sampled points off of each end of the data. The remaining signal had a maximum truncation error of  $|Dx - \dot{x}| < 2$ , where the maximum value of  $|\dot{x}|$  was about 161. The values of  $|Dx - \dot{x}|$  decreased monotonically (with an insignificant oscillation) as the index moved away from the endpoints toward the middle of the time record (Figure 1).

#### 4.0.1 Average Mutual Information

For determining a “good” choice of derivative order  $a$ , we looked at the average mutual information  $\bar{I}$  between  $x$  and  $D^a x$  as a function of  $a$ . The first minimum in the plot indicates that optimally independent coordinates for  $x$  and  $D^a x$  correspond to the case of  $a$  slightly less than 0.8, for which  $\bar{I} \approx 0.35$  (Figure 2, left graph). This is interesting, since, for oscillators, we might have expected  $a = 1$  such that the most independent coordinates are analogous to displacement and velocity (or current and voltage). A wide range of values of  $a$  provide lower average mutual information with  $x$  than the pair  $(x, D^2 x)$ .

In order to obtain several reconstruction coordinates without letting the average mutual information get “large,” and without letting the total order of the derivative get “large” so that the noise amplification is reasonable, we have chosen fractional derivative orders at multiples of  $a = 2/7$  for illustration of its use for phase-space reconstructions. For  $a = 2/7$  the average mutual information is slightly above one.

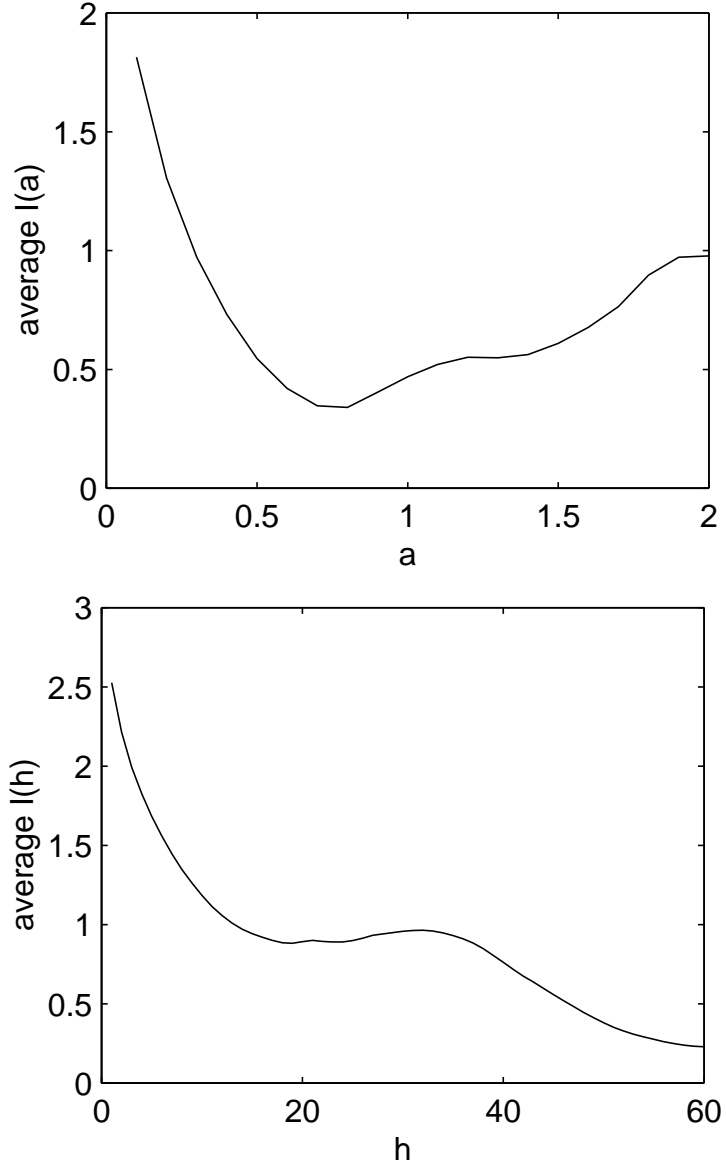


Figure 2: The left graph shows the average mutual information between the coordinates  $x$  and  $D^a x$  as a function of  $a$  for the Lorenz system. The right plot shows the average mutual information between delay coordinates  $x_n$  and  $x_{n+h}$  as a function of  $h$ .

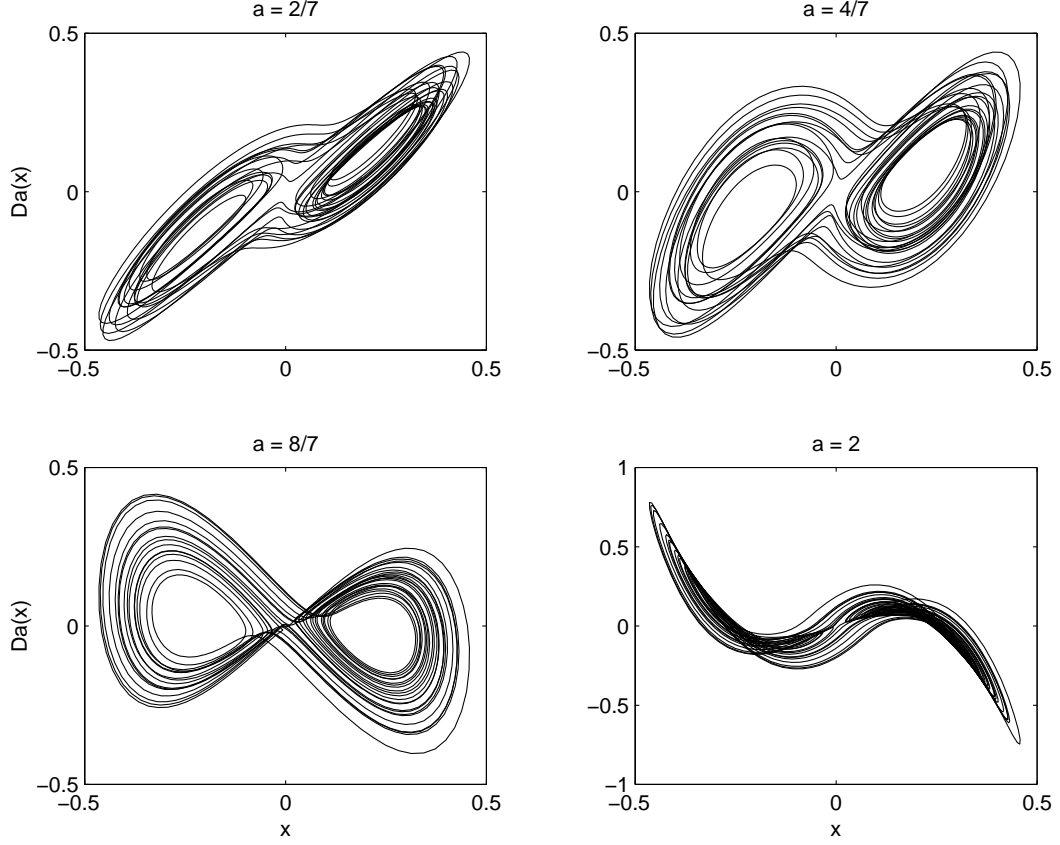


Figure 3: Plots of  $D^a x$  versus  $x$  for various values of  $a$  for the Lorenz system.

The values of mutual information surrounding the minimum for the fractional derivative pairs are quite competitive with those surrounding the local minimum in the method of delays (Figure 2, right-hand graph). The first local minimum for delay coordinates occurs at  $h = 19$ , with a value of about  $\bar{I} = 0.8$ . For a delay of  $h = 13$ , the  $\bar{I}$  between the delay pair is similar to the  $\bar{I}$  between the fractional derivative pair with  $a = 2/7$ .

#### 4.0.2 Reconstruction of the Phase Space

Figure 3 shows pseudo phase portraits involving the first three fractional derivatives of the signal  $x$  from the Lorenz system plotted against  $x$ , and also the plot of  $x$  vs.  $D^2 x$ .

The delay-space plots of the Lorenz system are shown in Figure 4. Close examination shows that, while the delay-space trajectories tend to locally define a sheet-like attracting set, i.e. a set of dimension that is close to two, the fractal-derivative-space trajectories seem less confined to a nearly two-dimensional sheet.

We look more closely at the fractional-derivative reconstructions of the Lorenz variable  $x$  with derivative orders of multiples of  $a = 2/7$ , in comparison with delay reconstructions with delays of  $h = 13$ , such that  $x_n$  and  $x_{n+h}$  are similarly independent as  $x(t)$  and  $D^a x(t)$ , according to Figure 2.

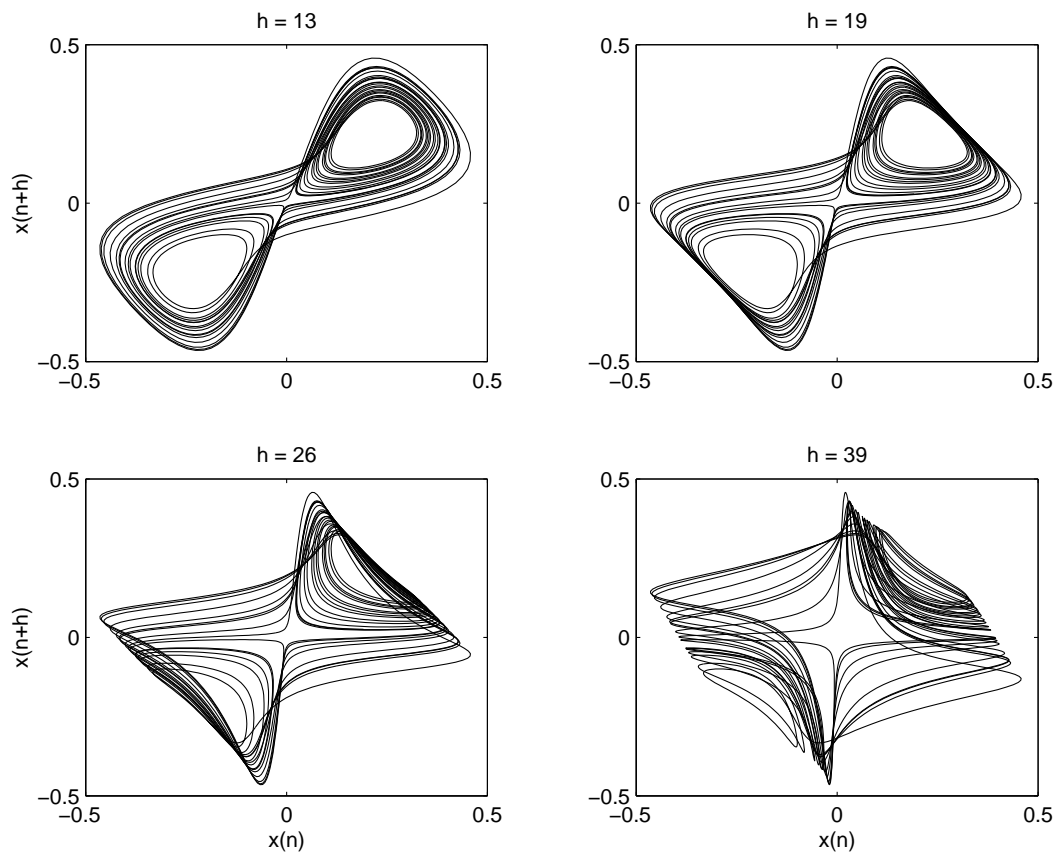


Figure 4: Plots of  $x_{n+h}$  versus  $x_n$  for various values of  $h$  for the Lorenz system.

For fractional-derivative reconstructions of the Lorenz variable  $x$  with orders of multiples of  $a = 2/7$ , the numbers of false nearest neighbors were 56695, 35416, 260, 0, 0, 0, 0, and 0, for reconstruction dimensions of one through eight. Since there are no FNNs at dimension four and above, we would be inclined to choose  $d_E = 4$  as the reconstruction dimension.

For the case of delay reconstructions with  $h = 13$ , for which the average mutual information matched that of the fractional derivative pair with  $a = 2/7$ , the numbers of false nearest neighbors were 56853, 4184, 0, 0, 0, 0, 0, and 0 for reconstruction dimensions of one through eight. Since there are no false nearest neighbors at dimension three or above, we can choose an embedding dimension  $d_E = 3$  to fully unfold the data.

Thus, the fractional derivative method with increments of  $a = 2/7$  did not unfold the data quite as efficiently as the method of delays with  $h = 13$ . However, the unfolding of the data is similar, being in the range of the expected reconstruction dimension, and is thus considered to be effective.

### 4.0.3 Characterization of the Data

Recurrence plots (Figure 5) indicate the numbers of recurrences at various values of delay indices. The plots show that the five-dimensional fractal derivative space and the true phase space produce qualitatively similar recurrence behavior for the same response data, in terms of the widths and locations of the recurrence bands. The true phase space reveals more recurrences for the period two and period three unstable periodic orbits. When a recurrence is found in both spaces, it occurs at nearly the same index. Hence, the fractional-derivative leads to little distortion in the temporal location of recurrences.

Finally, we computed the correlation dimension,  $d_c$ , by computing the correlation integral  $C(r)$  for various ball sizes,  $r$ , based on 1000 randomly chosen reference points in the data (but the same reference indices for each reconstruction).

The correlation dimensions were  $d_c = 1.89$  for the true phase space,  $d_c = 2.52$  for the fractional-derivative phase space, and  $d_c = 2.01$  for the delay reconstruction. The fractal dimension (limit capacity) of this system is known to be slightly above two, and the correlation dimension is a lower bound to the limit capacity [24, 25]. The large deviation of the correlation dimension for the fractional derivative is consistent with the previous observation that the reconstructed trajectories look more tangled, and less sheet-like, in the fractional derivative space.

To further investigate what is going on here, we looked at the Poincaré sections constructed by plotting two of the phase-variable values at the instant the true  $z$  variable crossed upward through the value of 25 (about which there are oscillations in the  $z$  variable). The Poincaré sections are shown in Figure 6.

The cross section of the attractor in the  $(x, Dx, z)$  space is nearly confined to a line. In fact, if we were to zoom in on the line, we would see a dense layering of Poincaré section points. However, as the order  $a$  of the derivative deviates from  $a = 1$ , the dense layering is disrupted. The case of  $a = 4/7$ , the furthest from  $a = 1$  of those plotted, shows the most deviation from the densely layered image. It is unknown whether this is a topologically equivalent expansion of the layering, or a more serious distortion of the geometry. The cases of  $a = 6/7$  and  $a = 8/7$  show slight expansion (note the scales of the plots are also expanded

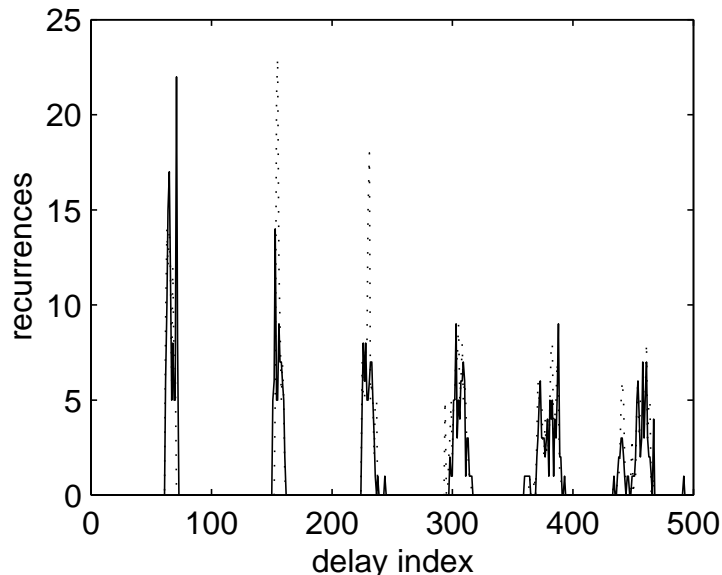


Figure 5: The number of recurrences versus the delay index for of data from the Lorenz system. The solid line shows the recurrence plot from the fractional derivative reconstruction, and the dotted line shows the recurrence plot from the true phase space.

compared to the case of  $a = 1$ .)

Some comments are needed. The fractional derivative, when computed in the frequency domain by using the FFT, involves a multiplication by  $(i\omega)^a$ . In comparison to the case of  $a = 1$ , the simple derivative, the case of  $0 < a < 1$  more heavily weighs the low frequency content of the signal, and the case of  $a > 1$  more heavily weighs the high-frequency content of the signal. For the case of  $0 < a < 1$ , added emphasis on the low frequency components “slows down” the effect of the derivative.

Let us imagine, for example, a saturated sine wave,  $x_s(t)$ , which is constant over the time intervals of saturation. The simple derivative  $\dot{x}_s(t)$  will have zero values over the time intervals of saturation. The trivial case of the derivative  $D^a x_s(t)$  where  $a = 0$  will have constant values over the intervals of saturation. It turns out that over a continuous change in values of  $a$  from zero to one, there is a continuous change from having constant to zero values over the intervals of saturation. In the intervals of saturation,  $D^a x_s(t)$  is neither zero nor constant, but changing in time. A plot of the fractional derivatives of a square wave, shown in Oldham and Spanier [35], also exhibits this effect. From this perspective, it might seem that dynamics are added to the signal. However, for a new state to be added, the reconstructed coordinate, say  $\phi$ , should have additional dynamics, such that  $D^a \phi = f(\mathbf{x}, \phi)$ . However, the fractional derivative with  $a > 0$  would add a zero (to the transfer function of a linear system) rather than a pole, and apparently preserve the number of dynamic states. This issue needs further investigation.

Furthermore, in tests of isolated segments of the Lorenz response data, we find that, as calculated with the FFT, the fractional derivative at an instant is dependent on the

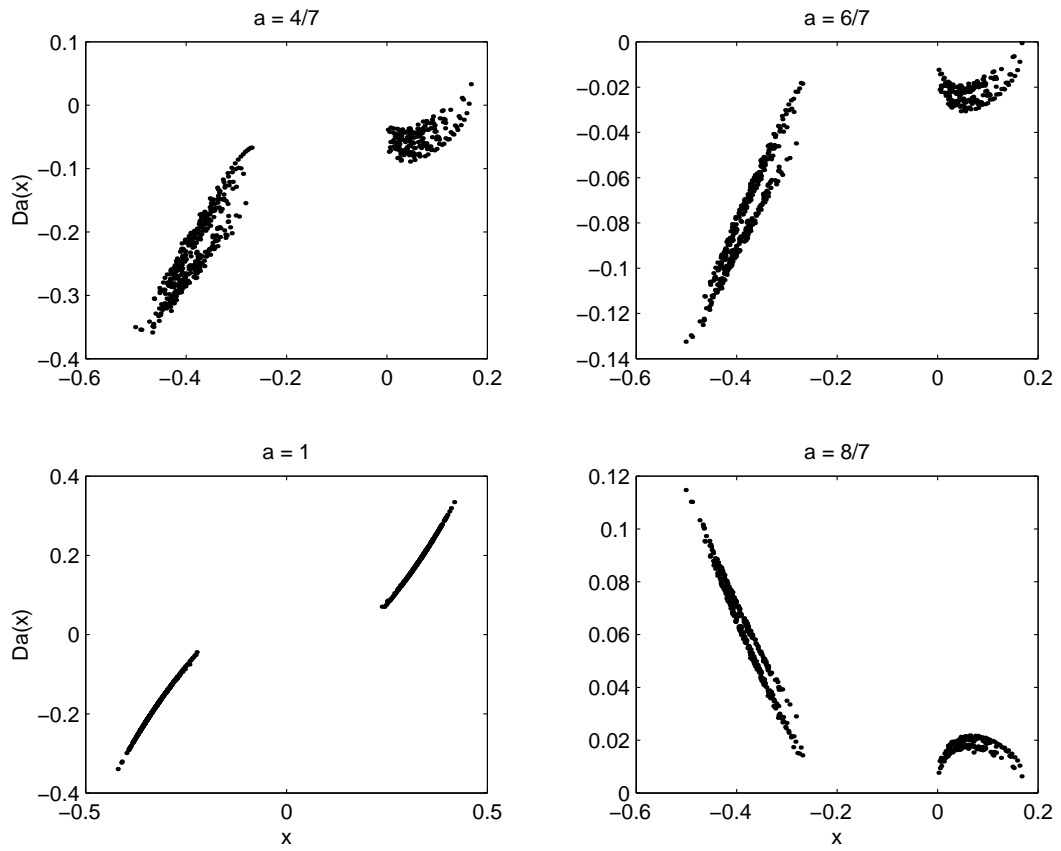


Figure 6: Poincaré sections of  $D^a(x)$  versus  $x$  for various values of  $a$  for the Lorenz system. The points were generated as the true state variable  $z$  crossed upward through the value 25.



past and future history of the signal. The future dependence makes the operation non causal, perhaps a property of the frequency-domain computation, which is acceptable for post processing. Past history dependence is not surprising since the definition equation (2) involves an integral. This history dependence puts in jeopardy the previously asserted advantage of instantaneity in time. The history dependence could also affect the locations of extracted unstable periodic orbits. Should the same unstable periodic orbit be visited twice, but surrounded by completely different trajectories each time, is it possible that the location of the extracted periodic orbit might vary with the surrounding history. This also needs investigation.

## 5 Conclusion

We have proposed the use of fractional derivatives as a means of reconstructing the phase space of low-dimensional nonlinear dynamical systems. The idea is that the fractional derivative of a signal provides an otherwise independent signal. The order of the fractional derivative is a parameter in the reconstruction, analogous to the delay index in delay reconstructions. The fractional order was chosen rather qualitatively to minimize the total derivative order, and hence the noise amplification, in the reconstruction coordinates, while examining the average mutual information to keep the first coordinate pair sufficiently independent.

The fractional derivatives successfully unfolded the phase space in the Lorenz system, based on the FNN test. The resulting embedding dimension was within one dimension of the result for delay embeddings of the same data.

The search for unstable periodic orbits in the fractional-derivative pseudo phase space and the true phase space produced similar recurrence plots. Indeed, the indices of commonly recurrent trajectories were similar, indicating the same unstable periodic orbits are likely to be extracted in either phase space.

The correlation dimensions were computed in the fractional derivative reconstruction, the delay reconstruction, and the true phase space. It is rare for such characterizations to be performed in a reconstruction other than a delay embedding [14]. The correlation dimension in the fractional derivative reconstruction differed from the true phase space, although it was still in a range that would represent qualitative similarity. There is some history dependence in the fractional derivative. Whether this is detrimental for its use as a reconstruction tool is not yet determined.

The fractional derivative method is simple, requiring simple Matlab code, for example. In truth, the method of delays is more simple, and is expected to continue as the preferred method. However, the fractional derivative method provides a valuable tool, and is likely to find applications. For example, the fractional derivative history dependence should provide a “cure” for the phase space collapse seen in delay reconstructions of stick-slip signals [12, 15]. This should be studied. Generally, the reconstruction will be useful for analyses (such as modeling, identification and prediction) of long time-series data that are facilitated by unfolding the data in a higher-dimensional phase space. Applications are broad, and could include engineering oscillations, biological dynamics, economics and climate studies. It would be of interest to seek a mathematical proof of the ability of fractional derivative

reconstructions to perform embeddings.

## Acknowledgements

We are thankful to: the NASA-Langley Research Center (grant number NAG-1-01048), with Dr. Walt Silva; the National Science Foundation (GOALI grant number DMII-9800323).

## References

- [1] Kennel, M., Brown, R., and Abarbanel, H. D. I., 1992, “Determining embedding dimension for phase-space reconstruction using a geometrical construction,” *Physical Review A* **45**, 3403-3411.
- [2] Abarbanel, H. D. I., Brown, R., Sidorowich, J., and Tsimring, L. (1993) “The analysis of observed chaotic data in physical systems,” *Reviews of Modern Physics* **65**, 1331-1392.
- [3] Takens, F. (1981) “Detecting strange attractors in turbulence,” *Lecture Notes in Mathematics* **898**, Springer, 366-381.
- [4] Packard, N. H., Crutchfield, J. P., Farmer, J. D., and Shaw, R. S., 1980, “Geometry from a time series,” *Physical Review Letters* **45** (9) 712-716.
- [5] Noakes, L., 1991, “The Takens Embedding Theorem,” *International Journal of Bifurcation and Chaos* **1** (4) 867-872.
- [6] Fraser, A. M. (1989) “Reconstructing attractors from scalar time series: a comparison of singular system analysis and redundancy criteria,” *Physica D* **34**, 391-404.
- [7] Ravindra, B. (1998) “Comments on On the physical interpretation of proper orthogonal modes in vibrations,” *Journal of Sound and Vibration*, to appear.
- [8] A. M. Fraser and H. L. Swinney, 1986, “Independent coordinates for strange attractors from mutual information,” *Physical Review A* **33** (2), 1134-1140.
- [9] Cao, L., 1997, “Practical Method for Determining the Minimum Embedding Dimension of a Scalar Time Series,” *Physica D* **110** 43-50.
- [10] Potopov, A., 1997, “Distortions of Reconstruction for Chaotic Attractors,” *Physica D* **101** 207-226.
- [11] Mindlin, G. B., and Solari, H. G., 1995, “Topologically Inequivalent Embeddings,” *Physical Review E* **52** (2) 1497-1502.
- [12] B. F. Feeny and J. W. Liang, 1997, “Phase-space reconstructions and stick-slip,” *Nonlinear Dynamics* **13** (1), 39-57.

- [13] Gilmore, R., 1998, "Topological Analysis of Chaotic Dynamical Systems," *Review of Modern Physics* **70** (4) 1455-1526.
- [14] Gilmore, R. and Lefranc, M., 2002, *The Topology of Chaos*, Wiley-Interscience, New York.
- [15] Lin, G., 2001, *Phase-Space Reconstruction by Alternative Methods*, M.S. Thesis, Michigan State University, East Lansing.
- [16] Auerbach, D., Cvitanovic, P., Eckmann, J.-P., Gunaratne, G., and Procaccia, I. (1987) "Exploring chaotic notion through periodic orbits," *Physical Review Letters* **58**, 2387.
- [17] Lathrop, D. P. and Kostelich, E. J. (1989) "Characterization of an experimental strange attractor by periodic orbits," *Physical Review A* **40**, 4028.
- [18] Tufillaro, N. B., Abbott, T., and Reilly, J. (1992) *An Experimental Approach to Nonlinear Dynamics and Chaos*, Addison-Wesley, New York.
- [19] Grebogi, C., Ott, E., and Yorke, J. [1988] 'Unstable periodic orbits and the dimensions of multifractal chaotic attractors,' *Physical Review A* **37**(5) 1711-1724.
- [20] Kesaraju, R. V. and S. T. Noah (1994) *Nonlinear Dynamics* **6**, 433-457. Characterization and detection of parameter variations of nonlinear mechanical systems.
- [21] Van de Wouw, N., Verbeek, G., and Van Campen, D. H., 1995, "Nonlinear parametric identification using chaotic data," *Journal of Vibration and Control* **1**, 291-305.
- [22] Yuan, C.-M., and B. F. Feeny (1998) "Parametric identification of chaotic systems," *Journal of Vibration and Control* **4**(4) 405-426.
- [23] Feeny, B. F. C.-M. Yuan and J. P. Cusumano, 2001, "Parametric identification of an experimental two-well oscillator," *Journal of Sound and Vibration* **247**(5) 785-806.
- [24] Gerschenfeld, N. (1988) "An Experimentalist's Introduction to the Observation of Dynamical Systems," in *Directions in Chaos*, Vol. II, Hao Bai-Lin (ed.), World Scientific, Singapore.
- [25] Feder, J. (1988) *Fractals* (Plenum Press, New York).
- [26] Feeny, B. F. (2000) "Fast multifractal analysis by recursive box-covering," *International Journal of Bifurcations and Chaos* **10**(9) 2277-2287.
- [27] Grassberger, P., and Procaccia, I., (1983) "Characterization of Strange Attractors," *Physical Review Letters* **50** 346-349.
- [28] Malraison, G., Atten, P., Berge, P., and Dubois, M., (1983) "Dimension of Strange Attractors: An Experimental Determination of the Chaotic Regime of Two Convective Systems," *Journal of Physics Letters* **44** 897-902.

- [29] Cusumano, J. P. (1990) *Low-Dimensional, Chaotic, Nonplanar Motions of the Elastica: Experiment and Theory*, PhD Thesis, Cornell University, Ithaca.
- [30] Bagley, R. L. and Calico, R. A., 1991, "Fractional Order State Equations for the Control of Viscoelastically Damped Structures," *AIAA Journal of Guidance*, **14** (2) 304-311.
- [31] Padovan, J. and Sawicki, J. T., 1998, "Nonlinear Vibrations of Fractionally Damped Systems," *Nonlinear Dynamics* **16** (4) 321-336.
- [32] Zhang, W., and Shimizu, N., 1998, "Numerical Algorithm for Dynamic Problems Involving Fractional Operators," *JSME International Journal, Series C*, **41** (3) 364-370.
- [33] He, J. H., 1998, "Approximate Analytical solution for Seepage Flow with Fractional Derivatives in Porous Media," *Computational Methods in Applied Mechanics and Engineering* **167** 57-68.
- [34] Stiasnie, M., 1997, "A Look at Fractal Functions through their Fractional Derivatives," *Fractals* **5** (4) 561-564.
- [35] Oldham, K. B. and Spanier, J., 1974, *The Fractional Calculus. Theory and Application of Differentiation and Integration to Arbitrary Order*, Academic Press, New York and London.
- [36] Beran, J., 1994, *Statistics for Long-Memory Processes*, Chapman and Hill, London.
- [37] Baillie, R. T., 1996, "Long memory processes and fractional integration in econometrics," *Journal of Econometrics* **73**(1) 5-59.
- [38] Tseng, C.-C., Pei, S.-C., Hsia, S.-C., 2000, "Computation of Fractional Derivatives using Fourier Transform and Digital FIR Differentiator," *Signal Processing* **80** 151-159.
- [39] Ewins, D. J., 1984, *Modal Testing: Theory and Practice*, Research Studies Press, Letchworth, Hertfordshire, England.
- [40] Feeny, B. F. and Lin, G., 2003, "Reconstructing the Phase Space with Fractional Derivatives," ASME International Design Engineering Technical Conferences, Chicago, September 2-6, on CD-ROM.
- [41] Lorenz, E. N. 1963, "Deterministic Nonperiodic Flow," *Journal of Atmospheric Science* **20** 130-141.